J. Cent. South Univ. (2021) 28: 2947−2960
DOI: https://doi.org/10.1007/s11771-021-4818-3

Springer

Sound absorption performance of acoustic metamaterials composed of double-layer honeycomb structure

WANG Da(王达)[1, 2, 3, 4], XIE Su-chao(谢素超)[1, 2, 3]*, YANG Shi-chen(杨诗晨)[1, 2, 3], LI Zhen(李臻)[1, 2, 3]

1. Key Laboratory of Traffic Safety on Track of Ministry of Education, Changsha 410075, China;
2. Joint International Research Laboratory of Key Technology for Rail Traffic Safety, Changsha 410075, China;
3. School of Traffic & Transportation Engineering, Central South University, Changsha 410075, China;
4. National Innovation Center of Advanced Rail Transit Equipment, Zhuzhou 412001, China

Abstract: The purpose of the research is to assess the sound absorption performance (SAP) of acoustic metamaterials made of double-layer Nomex honeycomb structures in which a micro-orifice corresponds to a honeycomb unit. For this purpose, the influences of structural parameters on the SAP of acoustic metamaterials were investigated by using experimental testing and a validated theoretical model. In addition, the sandwich structure was optimized by the genetic algorithm. The research shows that the panel thickness and micro-orifice diameter mainly affect the second resonant frequency and second peak sound absorption coefficient (SAC) of the structure. The unit cell size is found to influence the first and second resonant frequencies and two peaks of the SAC. An extremely low side-length of the honeycomb core decreases the SAP of the structure for low-frequency noise signals. Additionally, the sandwich structure presents a better SAP when the diameter of micro-orifices on the front micro-perforated panel (MPP) exceeds that of the back MPP. The sandwich structure shows better noise reduction performance after the optimization aiming at the noise frequency outside trains.

Key words: acoustic metamaterials; sound absorption; honeycomb sandwich panel; micro-perforated panel

Cite this article as: WANG Da, XIE Su-chao, YANG Shi-chen, LI Zhen. Sound absorption performance of acoustic metamaterialscomposed of double-layer honeycomb structure [J]. Journal of Central South University, 2021, 28(9): 2947−2960. DOI: https://doi.org/10.1007/s11771-021-4818-3.

1 Introduction

Traditional sound absorption materials are generally porous and air-permeable: pores on the material surface allow sound waves to be easily transmitted into the materials [1], however, a thickness equivalent to the length of sound waves is generally required for porous materials to realize favorable sound absorption. To absorb low-frequency and medium-frequency sound waves, porous materials require to be at least 30 to 50 mm thick [2]. Porous materials, generally soft, do not exhibit enhanced mechanical properties while increasing their mass, which greatly restricts their practical application. Traditional acoustic materials (AMs) suffer drawbacks such as large volume and mass and thus they cannot satisfy the current

Foundation item: Project(51775558) supported by the National Natural Science Foundation of China; Project(2019JJ30034) supported by the Natural Science Foundation for Excellent Youth Scholars of Hunan Province, China; Project(20181053303gg) supported by the Training Objects of Young-Middle-Aged Backbone Teacher in Ordinary Universities of Hunan Province, China
Received date: 2021-01-23; **Accepted date:** 2021-03-08
Corresponding author: XIE Su-chao, PhD, Professor; E-mail: xsc0407@csu.edu.cn; ORCID: https://orcid.org/0000-0003-2855-2774

requirements for noise reduction, therefore, it is necessary to develop light-weight novel AMs with high stiffness and strength and favorable noise reduction.

With advantages including high specific strength, favorable impact resistance, and vibration reduction, the honeycomb sandwich structure and its composites have been widely applied in aerospace, railway vehicles, and buildings [3 − 5]. AMs fabricated by combining the honeycomb core with micro-perforated panels (MPPs) show enough mechanical strength and low mass. The MPP backed by a honeycomb structure can improve the sound absorption performance (SAP) of the MPP and enhance the absorption of medium and low-frequency noise [6−8]. Additionally, the honeycomb sandwich panels combine the AMs and supporting materials, thus improving space-utilization and convenience in design for noise reduction.

The investigation of the acoustic characteristics and the influences of structural parameters of honeycomb sandwich structure – MPPs composites are important when trying to replace the current types of AMs and improving the range of application.

The skin panels of a conventional honeycomb sandwich structure are generally compact materials, such as aluminum (Al) plate, so sound transmission is difficult. As a result, the SAP of the honeycomb structure worsens. Some scholars combine porous materials with honeycomb sandwich panels to improve the SAP of the honeycomb sandwich panels. LIN et al [9] designed a sandwich panel consisting of the polyethylene terephthalate (PET), TPU honeycomb, and polyurethane (PU) foam, which enables the sound absorption coefficient (SAC) of materials within 2 to 4 kHz to exceed 0.93. YANG et al [10] filled the honeycomb sandwich panel with glass fibers to increase the SAP of materials within 4 to 6.3 kHz. XIE et al [11] used polyester fibers to fill a composite honeycomb structure and the results showed that the composite structure presents a better SAP than that using polyester fibers of the same thickness.

The above research mainly concentrates on medium- and high-frequency noise. The sound absorption structures (such as perforation plate (PP), Helmholtz resonator (HR), and membrane resonator) based on resonators aiming at low-frequency noise have been investigated and used in practice [12, 13]. Academician MAA [14] first proposed the use of MPP, which shows an SAC of nearly 99% at the resonant frequency. Compared with traditional sound absorption materials, the MPP has a simple structure and can be applied under working conditions including high temperature and high pressure.

The MPP structure generally comprises the MPP and space at the back, in which the panel needs to be supported by the framework or the trimmer beam. The honeycomb core can satisfy the requirements imposed on stiffness and strength as well as supporting the space at the back of the MPP. The micro-perforated honeycomb panel consisting of the honeycomb core and MPPs demonstrates sufficient mechanical strength and low mass. Some scholars investigated the micro-perforated panel absorber (MPPA) backed by a honeycomb core [8]. TOYODA et al [6] found that it is possible to increase the peak of the SAC and reduce the corresponding peak frequency by reducing the thickness of the honeycomb wall. By measuring the SAP of MPPAs separately backed by an air layer and honeycomb structure, CHENG et al [7] suggested that the honeycomb core can control broadband noise. SAKAGAMI et al [15, 16] found that the honeycomb core can improve the SAP of the double-layer MPPs in the vicinity of the resonant peak and reduce their resonant frequency. Nevertheless, the above research only considers the holistic relationship between MPPs and the honeycomb core while failing to ascertain the relationship between the perforation and the cavity formed by honeycomb unit cells. Moreover, the structure fails to eliminate low-frequency noise and results in a fixed, narrow absorption peak due to its geometrical shape [17].

Aiming at the above problems, REGNIEZ et al [18] developed an impedance model with the honeycomb sandwich structure, in which a micro-perforation appears in each honeycomb unit. Afterwards, PENG et al [19] designed the periodically horizontally arranged composite honeycomb panels in which the honeycomb units contain perforations of different sizes, which can realize sound absorption from 600 to 1000 Hz. XIE

et al [20] found that a micro-perforated honeycomb metasurface panel is thinner and presents better sound absorption than the MPP at the same frequency. CHANG et al [21] showed that double-layer porous panels with a large depth of backing cavity deliver superior SAP within the low- and high-frequency ranges. JONZA et al [22] designed a panel, on the skin of which the honeycomb units are interactively connected with perforations to absorb noise at a specific frequency; moreover, the panel can absorb broadband noises on account of its multiple channel lengths and perforation sizes.

Above all, scholars have conducted research into the SAP of the honeycomb sandwich structures from many perspectives, and found that honeycomb sandwich panels show a certain superiority in AMs. The micro-perforated honeycomb panel consisting of the honeycomb core and MPPs exhibits favorable SAP. Through use of a multi-layer structure, it is feasible to significantly improve the SAP of the composite honeycomb structure by controlling the orifice diameter and cavity volume, however, the composite structure combining honeycomb sandwich panels and MPPs warrants further exploration. Most scholars fail to consider the positional relationship between the honeycomb unit cells and micro-perforations and the influence of multi-layer structure on the composite honeycomb structure.

Aiming at the above problems, the micro-perforations in MPPs separately correspond to unit cells of the honeycomb core, thus enabling the micro-perforations and honeycomb unit cells to form a resonator. Moreover, by exploiting the independence of the honeycomb unit cells, AMs with double-layer honeycomb sandwich panels were prepared by connecting honeycomb unit cells with different diameters of micro-perforations in series. Based on the theoretical model and experimental test, the influences of the thicknesses and orifice diameters of front and back panels as well as the size of honeycomb unit cells on the SAP of the composite structure were investigated. Based on the research results, the sandwich structure was optimized aiming at the main noise frequencies outside train carriages for use in urban rail transit systems to improve their noise reduction performance.

2 Theoretical model and test scheme for sound absorption of structure

2.1 Theoretical model for sound absorption based on transfer matrix method

In terms of the transfer matrix method, the loss of sound waves during propagation can be attained by solving the propagation relationship of sound waves in different media or acoustic impedances, to obtain the SAC of materials. Figure 1 shows the theoretical model of the double-layer Nomex honeycomb sandwich panel. The micro-perforations in MPPs separately correspond to unit cells of the honeycomb core, moreover, honeycomb unit cells with different diameters of micro-perforations are connected in series. The micro-perforations and honeycomb unit cells to form a resonator and the double-layer Nomex honeycomb sandwich panel comprise three layers, i.e., MPPs, an air layer, and the HR.

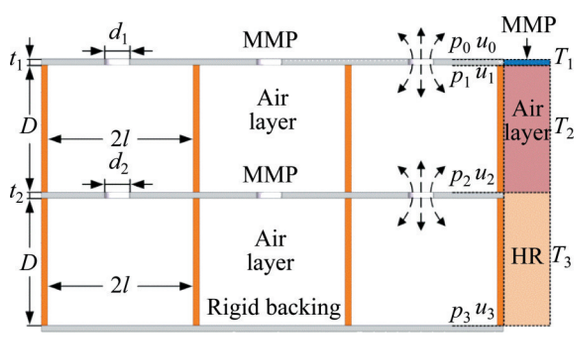

Figure 1 Theoretical model of double-layer honeycomb sandwich panel for sound absorption

The plane waves normally incident on the material surface reach the rigid backing through three layers of different media. Three transfer matrixes T_1, T_2 and T_3 are used to describe the relationships between state variables (acoustic pressure and particle velocity) at the incident surface and structural bottom. The MPP at the upper part is separated from the air cavity at the back because the air layer needs to be investigated alone owing to it being connected to the front and back MPPs. An HR is formed by using the second-layer MPP and the air cavity.

As shown on the right-hand side in Figure 1, it is supposed that the acoustic pressure and particle velocity on the structural incident surface are

separately expressed as p_0 and u_0; p_1 and u_1 denote the acoustic pressure and particle velocity after sound waves propagate through the MPP; the acoustic pressure and particle velocity after sound waves travel through the air layer are separately represented by p_2 and u_2; p_3 and u_3 represent the acoustic pressure and particle velocity at the rigid backing after the sound waves propagate through the HR, respectively. Therefore, the acoustic pressures and particle velocities in front and back of MPPs satisfy the following relationship:

$$\begin{bmatrix} p_0 \\ u_0 \end{bmatrix} = T_1 \begin{bmatrix} p_1 \\ u_1 \end{bmatrix} \tag{1}$$

where T_1 denotes the transfer matrix, which can be expressed as follows:

$$T_1 = \begin{bmatrix} A_{11} & A_{12} \\ A_{21} & A_{22} \end{bmatrix} \tag{2}$$

where A_{11}, A_{12}, A_{21} and A_{22} are unknowns representing the linear relationship between p_0, u_0 and p_1, u_1.

It is supposed that plane waves propagate in front and back of the MPPs and the medium is isotropic. According to the condition of continuity of the velocity at boundaries, u_0=u_1. The acoustic impedance ratio of the MPP is such that $z_{\mathrm{M}} = r_{\mathrm{MPP}} + \mathrm{j}\omega m_{\mathrm{MPP}}$, among them, r_{MPP} is the real part and ωm_{MPP} is the imaginary part. The acoustic impedance ratio (in acoustic terms) is defined as follows:

$$z_{\mathrm{M}} = \frac{p_0 - p_1}{u_0} = \frac{p_0 - p_1}{u_1} \tag{3}$$

That is, $p_0 = p_1 + u_0 z_{\mathrm{M}}$ and $u_0 = u_1$, and thus matrix T_1 in Eq. (2) is also expressed as follows:

$$T_1 = \begin{bmatrix} A_{11} & A_{12} \\ A_{21} & A_{22} \end{bmatrix} = \begin{bmatrix} 1 & z_{\mathrm{M}} \\ 0 & 1 \end{bmatrix} \tag{4}$$

In a similar way, the transfer matrix T_2 for the air layer at back of the MPP can be expressed as follows:

$$\begin{aligned} T_2 &= \begin{bmatrix} B_{11} & B_{12} \\ B_{21} & B_{22} \end{bmatrix} \\ &= \begin{bmatrix} \cos\left(kD_1\right) & \mathrm{j}\rho_0 c_0 \sin\left(kD_1\right) \\ \mathrm{j}\sin\left(kD_1\right)/\rho_0 c_0 & \cos\left(kD_1\right) \end{bmatrix} \end{aligned} \tag{5}$$

where ρ_0, c_0 and D denote the air density, the propagation velocity of sound waves in air, and the depth of the air cavity, respectively; it is assumed that only sound waves propagate in the medium, u_0 can be neglected for k, so $k = \omega/c_0$ stands for the number of sound waves, where ω refers to the angular frequency[23].

An HR is formed by combining the second-layer MPP with the air cavity at the back, whose transfer matrix T_3 is as follows:

$$T_3 = \begin{bmatrix} C_{11} & C_{12} \\ C_{21} & C_{22} \end{bmatrix} = \begin{bmatrix} 1 & z_{\mathrm{HR}} \\ 0 & 1 \end{bmatrix} \tag{6}$$

The acoustic impedance ratio of the HR is such that $z_{\mathrm{HR}} = r_{\mathrm{HR}} + \mathrm{j}x_{\mathrm{HR}}$, among them, r_{HR} is the real part and x_{HR} is the imaginary part.

In the double-layer honeycomb sandwich plane structure, series multiplication is performed on the transfer matrixes of various units according to the propagation order of sound waves to obtain the total transfer matrix T:

$$T = T_1 T_2 T_3 = \begin{bmatrix} T_{11} & T_{12} \\ T_{21} & T_{22} \end{bmatrix} \tag{7}$$

According to the total transfer matrix of the honeycomb sandwich structure, the relationship between state variables (acoustic pressure and particle velocity) of the incident surface and the structural bottom is described as follows:

$$\begin{bmatrix} p_0 \\ u_0 \end{bmatrix} = \begin{bmatrix} T_{11} & T_{12} \\ T_{21} & T_{22} \end{bmatrix} \begin{bmatrix} p_3 \\ u_3 \end{bmatrix} \tag{8}$$

Owing to the particle velocity being zero at the rigid backing, that is, $u_3 = 0$, the acoustic impedance ratio of the structural surface is given by $z_{\mathrm{s}} = \dfrac{p_0}{u_0} = r_{\mathrm{s}} + \mathrm{j}x_{\mathrm{s}}$. By substituting Eqs. (4)–(6) into Eq. (8), the acoustic impedance ratio of the structural surface is given by [21]:

$$z_{\mathrm{s}} = z_{\mathrm{M}} + \frac{z_{\mathrm{HR}} \cos\left(\omega D_1/c_0\right) + \mathrm{j}\sin\left(\omega D_1/c_0\right)}{\cos\left(\omega D_1/c_0\right) + \mathrm{j}z_{\mathrm{HR}} \sin\left(\omega D_1/c_0\right)} \tag{9}$$

Based on theories proposed by YANG et al [24] and BAI et al [25], the acoustic impedance ratio of the MPP is

$$z_{\mathrm{MPP}} = r_{\mathrm{MPP}} + \mathrm{j}\omega m_{\mathrm{MPP}} \tag{10}$$

$$r_{\mathrm{MPP}} = \frac{32(\mu + \upsilon)t}{c_0 \varepsilon d^2}\left(\sqrt{1 + \frac{K^2}{32}} + \frac{\sqrt{2}\,Kd}{8t}\right) \tag{11}$$

$$m_{\mathrm{MPP}}=\frac{t}{c_0\varepsilon}\left(1+\frac{1}{\sqrt{9+K^2/2}}+0.85\frac{d}{t}\right) \tag{12}$$

where d, t, μ and υ refer to the orifice diameter of the MPP, the thickness of the MPP, the coefficient of kinematic viscosity of air (1.506×10^{-5} m^2/s), and the temperature coefficient of conductivity (2.0×10^{-5} m^2/s), respectively; $K=\frac{d}{2}\sqrt{\frac{\omega}{\mu}}$ and ε denote the constant of the MPP and perforation rate (the ratio of the perforated area to the total panel area), respectively.

At the third-layer, the micro-perforations in MPPs separately correspond to unit cells of the honeycomb core, and from Refs. [19, 20], it can be deduced that the HR model can provide better predictions of the experimental results than an MPP model. Based on the theoretical model by PENG et al [19] and XIE et al [20], the unit cells of the honeycomb sandwich panel covered by the MMP are equivalent to HR with the cylindrical concentric neck. The acoustic impedance ratio of the HR can be expressed as follows:

$$z_{\mathrm{HR}}=r_{\mathrm{HR}}+\mathrm{j}x_{\mathrm{HR}} \tag{13}$$

$$r_{\mathrm{HR}}=\frac{k}{\varepsilon d}\left[2\sigma_{\mathrm{v}}t_{\mathrm{eff}}+(\gamma-1)\sigma_{\mathrm{t}}t\right] \tag{14}$$

$$x_{\mathrm{HR}}=\frac{kt_{\mathrm{eff}}}{\varepsilon}\left(1+\frac{2\sigma_{\mathrm{v}}}{d}\right)-\mathrm{j}\cot(kD) \tag{15}$$

where $k=\omega/c_0$, $\sigma_{\mathrm{v}}=\sqrt{2\mu/\omega}$, and $\gamma=1.4$ represent the number of sound waves, the thickness of the viscous boundary layer and Poisson ratio of air, respectively; $\sigma_{\mathrm{t}}=\sqrt{2H/\rho_0C_p\omega}\approx\frac{0.25\times10^{-2}}{\sqrt{f}}$ denotes the thickness of the thermal boundary layer, in which f, H, and C_p separately refer to the frequency, thermal conductivity, and the specific heat capacity of air under constant pressure; t_{eff} denotes the effective length considering the acoustic radiation in the end of micro-perforations and interaction between micro-perforations.

The actual micro-perforated honeycomb sandwich panel forms a finite boundary. Considering the effects of the orifice diameter at the boundary and the honeycomb core at the back, PENG et al [19] replaced the perforation rate ε of the micro-perforated honeycomb sandwich panel with the effective perforation rate $\varepsilon_{\mathrm{eff}}$, with $\varepsilon_{\mathrm{eff}}=\varepsilon/\phi$, where ϕ denotes the correction coefficient.

This assumes that a plane wave is normally incident on an infinite plane with an acoustic impedance ratio z_{s} equal to that of the honeycomb sandwich structure. The pressure reflection coefficient r can be estimated by $r=(z_{\mathrm{s}}-1)/(z_{\mathrm{s}}+1)$ with absorption coefficient $\alpha=1-|r|$ [26]. Then the SAC of honeycomb sandwich structure can be expressed as follows:

$$\alpha=\frac{4r_{\mathrm{s}}}{(1+r_{\mathrm{s}})^2+(x_{\mathrm{s}})^2} \tag{16}$$

2.2 Test samples and scheme

According to ASTM E1050-08, the test was conducted at a relative humidity of (65±2)% at room temperature (20±1) °C. Through use of an impedance-tube test with two microphones, the SAC of the samples was assessed and the impedance tube for the test can be used at frequencies of 63−6300 Hz. In the impedance-tube test, the samples were sealed with a dense flexible sealant because the gaps around the edge of the samples exert significant influences on the measured SAC. During the test, the samples were sealed by applying polytetrafluoroethylene tape to avoid leakage of sound caused by surrounding cracks or gaps.

The test samples are shown in Figure 2. The MPP was made from polyvinyl chloride (PVC) and the honeycomb core was a Nomex honeycomb. The MPPs were bonded with the honeycomb core using resin. The influences of the orifice diameters of front and back MPPs on the SAP of the structure were investigated experimentally.

Afterwards, the effectiveness and accuracy of the theoretical model of the double-layer honeycomb sandwich panel for sound absorption were validated according to the test results.

Table 1 lists the salient dimensional parameters of the specimens used for the test.

3 Analysis of test results and influence of each parameter

The reproducibility results obtained for Test number 1 are shown in Figure 3, the trends observed

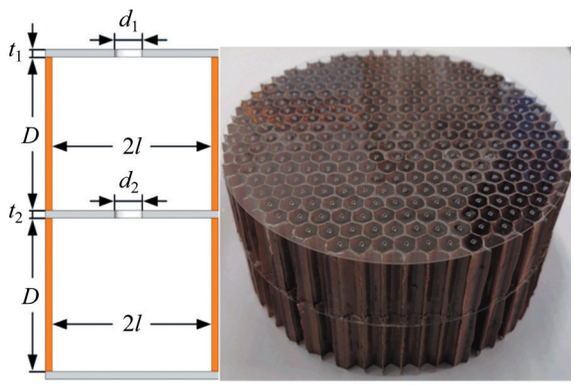

Figure 2 Specimen for double-layer honeycomb sandwich panel testing: (a) Structural parameters of double-layer honeycomb sandwich panel; (b) Samples of double-layer honeycomb sandwich panel

Table 3 Parameters of SAC test specimens of double-layer honeycomb sandwich panel

Test number	d_1/mm	d_2/mm	t_1=t_2/mm	D/mm	l/mm
1	0.4	0.7			
2	0.5	0.7			
3	0.6	0.7			
4	0.7	0.7	0.3	20	2.75
5	0.7	0.6			
6	0.7	0.5			
7	0.7	0.4			

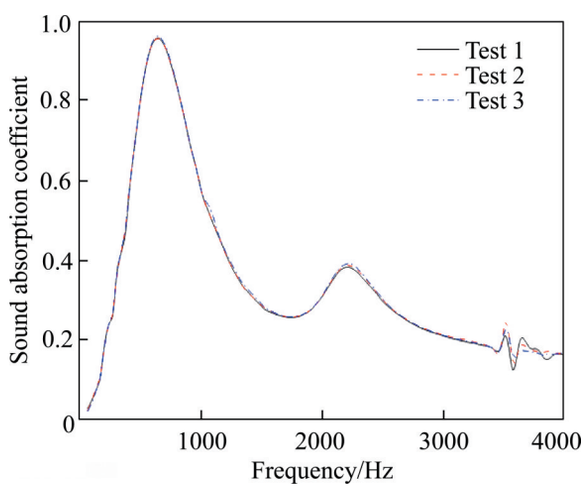

Figure 3 Reproducibility of Test number 1

in the SAC curves are essentially consistent between tests. This implies that the specimens and the tube are indeed well sealed and that the test results obtained are experimentally reproducible and reliable.

3.1 Influences of orifice diameters d_1 and d_2 of front and back MPPs on SAC

Figure 4(a) compares the SAC curves of the honeycomb sandwich structure with different orifice diameters of the front MPP. The amplitude of the second peak of the SAC increases with the growth of the orifice diameter of the front MPP. The first peaks of the SAC of the structure are all greater than 0.95. The second peak of the SAC reaches about 0.78 when the orifice diameter of the front MPP is identical to that of the back MPP. With the two peaks of the SAC, the sound absorption bandwidth of the double-layer structure is larger than that of the single-layer panel, however, the overall SAP of the double-layer structure is influenced by the extremely low second peak of the SAC.

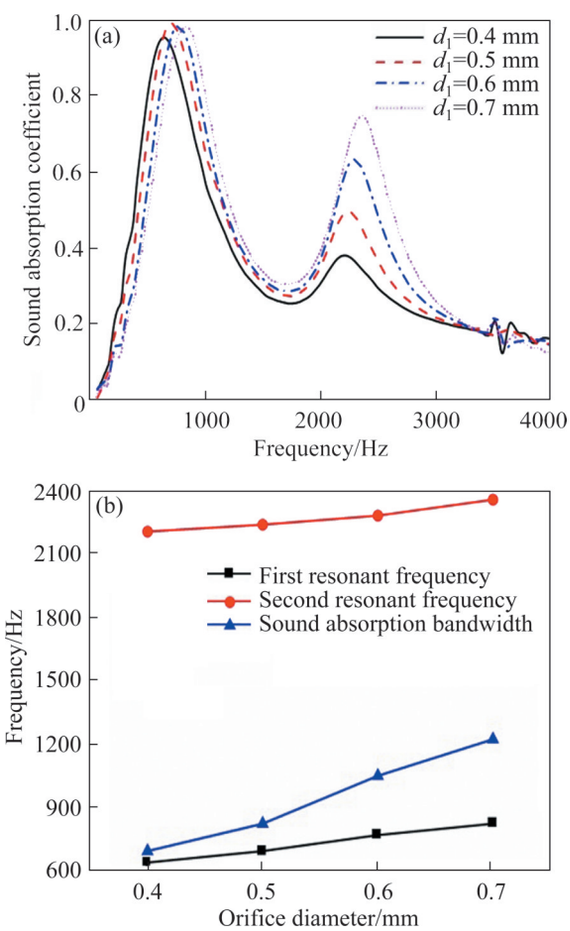

Figure 4 Influences of orifice diameter of front MPP on SAC (experiment): (a) Frequency – SAC; (b) Orifice diameter with resonant frequency and bandwidth

The theoretical value of the sound absorption bandwidth of the materials is determined as the width between two frequency points corresponding to the half of the maximum SAC of the structure. To

better show the SAP of such materials, the width between two frequency points corresponding to an SAC of 0.5 is generally used.

As shown in Figure 4(b), with increasing orifice diameter of the front MPP, the first frequency increases and the second resonant frequency increases (albeit to a lesser extent). The SACs near the second peak increase due to the growth of the second peak of the SAC, therefore, the sound absorption bandwidth of the structure with the SAC exceeding 0.5 increases to a significant extent, causing the sound absorption bandwidth of the structure to increase.

As shown in Figure 5(a), by comparing the SAC curves of the structure with different orifice diameters of the back MPP, it can be found that the amplitude of second peak of the SAC decreases with the growth of the orifice diameter of the back MPP. Figure 5(b) illustrates the influences of the orifice diameter of the back MPP on the resonant frequency and frequency bandwidth of the structure. The result shows that with increasing orifice diameter, the first and the second resonant frequency increases and the first resonant frequency increases (albeit to a lesser extent). At an orifice diameter of the back MPP of 0.4 and 0.5 mm, the structure presents a large sound-absorption bandwidth of about 1800 Hz, however, the sound absorption bandwidth decreases once the orifice diameter of the back MPP decreases to less than 0.6 mm because the wave trough between the first and second peaks of SAC declines with the reduction of the second peak of the SAC. Therefore, the sound absorption bandwidth at an SAC that exceeds 0.5 decreases significantly, reducing the global sound absorption bandwidth of the structure.

Figures 6(a) and (b) show a comparison of the influences of the orifice diameters of the front and back MPPs on the SAC. It can be found that the second peak of the SAC of the double-layer

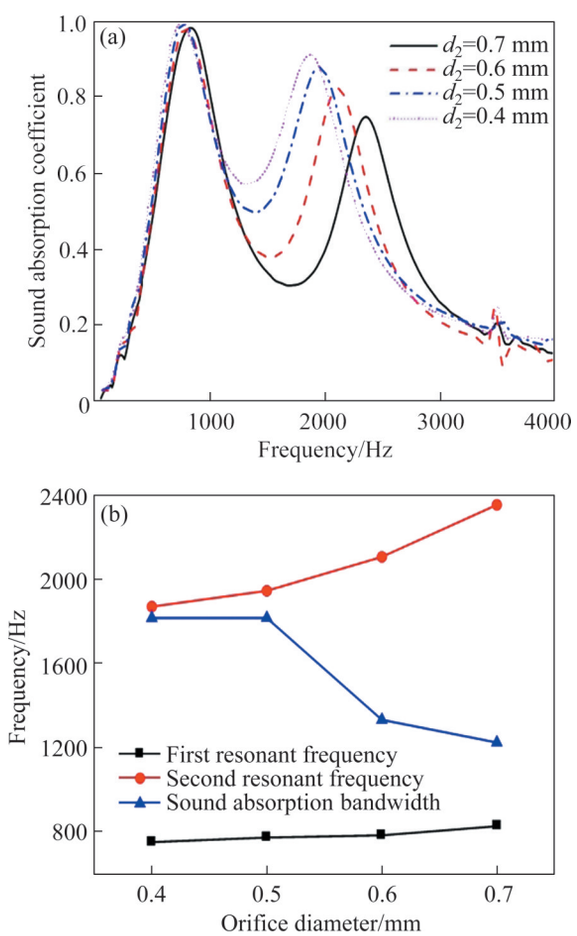

Figure 5 Influences of orifice diameters of back MPP on the SAC (experiment): (a) Frequency–SAC; (b) Orifice diameter with resonant frequency and bandwidth

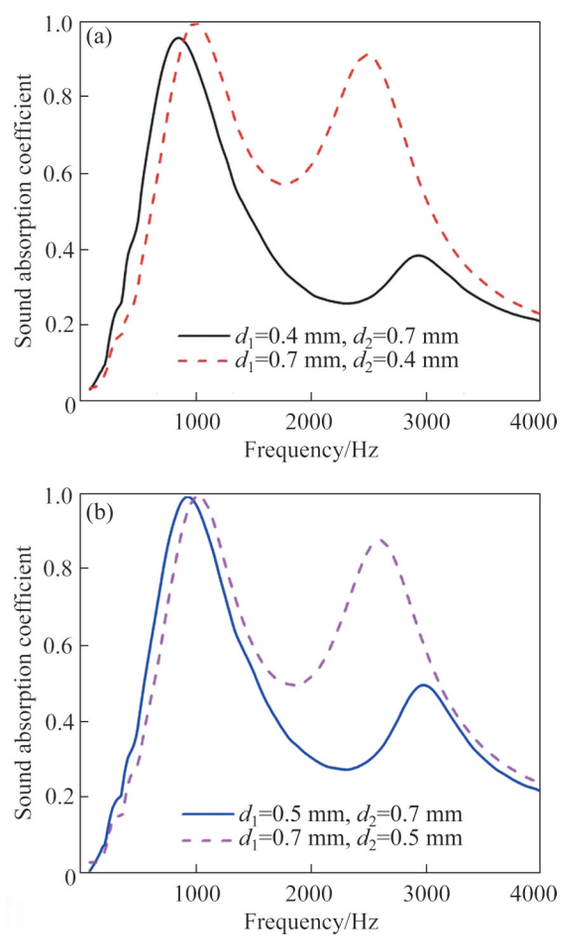

Figure 6 Influences of orifice diameters of front and back MPPs on SAC (experiment): (a) Orifice diameters of 0.4 and 0.7 mm; (b) Orifice diameters of 0.5 and 0.7 mm

structure when the orifice diameter of the front MPP is larger than that of the back MPP is much greater than that when the orifice diameter of the front MPP is lower than that of the back MPP.

Due to the series connection of two sets of resonators, two sound absorption peaks appear in the SAC curve of the structure, however, this combination of multiple resonators may be affected by coherent coupling effects or impedance mismatching, so different orders of arrangement will affect the SAP of the structure [27]. The second resonant frequency of the structure is lower, and the two resonant frequencies of the sound absorption curves tend to be closer. As a result, the double-layer structure shows a larger sound absorption bandwidth.

To validate the effectiveness and accuracy of the theoretical model based on the transfer matrix method, the results calculated using the theoretical model were compared with the test results, as shown in Figures 7(a) and (b). The theoretical result is consistent with the test result and the influences of the orifice diameters of the front and back MPPs on the SAC are also coincident. It indicates that the theoretical model is reliable. The visco-thermal effect within the honeycomb core and the HR cavity might be one of the causes of the deviations in the peak values and bandwidth of the absorption coefficients between the analysis and experiments [28, 29]. Due to the difficulty and accuracy of actual material processing, the influences of the MPP thickness and the side length of the honeycomb core on the SAC were analyzed based on the theoretical model.

3.2 Influences of thicknesses t_1 and t_2 of front and back MPPs on SAC

The other fixed geometric parameters of the structures are such that d_1=0.7 mm, d_2=0.6 mm, D=20 mm, and l=2.75 mm. In Figure 8(a) we can compare the curves of the SAC of the double-layer

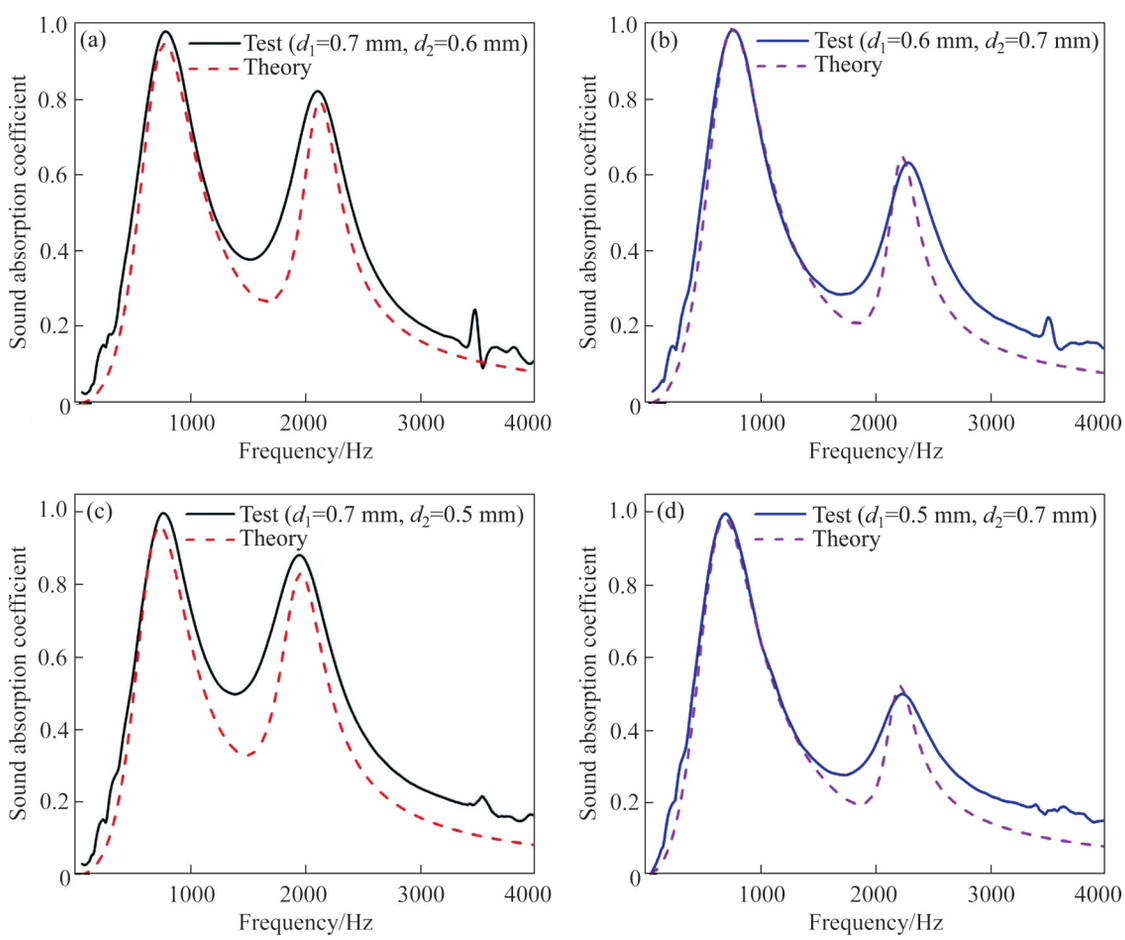

Figure 7 Comparison of curves of SAC obtained through test and theoretical prediction with different orifice diameters for front and back MPPs: (a) 0.7 and 0.6 mm; (b) 0.6 and 0.7 mm; (c) 0.7 and 0.5 mm; (d) 0.5 and 0.7 mm

structure with different thicknesses of the front MPP, showing the change law akin to that with different orifice diameters of the front MPP. The amplitude of the second peak of SAC decreases when increasing the thickness of the front MPP. The first peaks of the SAC all exceed 0.95 and are marginally affected by the change in the thickness of the front MPP. Figure 8(b) demonstrates the influences of the thickness of the front MPP on the resonant frequency and bandwidth of the double-layer structure. The thickness of the front MPP mainly influences the first resonant frequency, which decreases when increasing the thickness of the front MPP. Moreover, the second resonant frequency decreases only slightly as the thickness of the front MPP is increased. Owing to the amplitude of the second peak of the SAC decreasing with the increase in the thickness of the front MPP, the sound absorption bandwidth of the double-layer structure decreases globally.

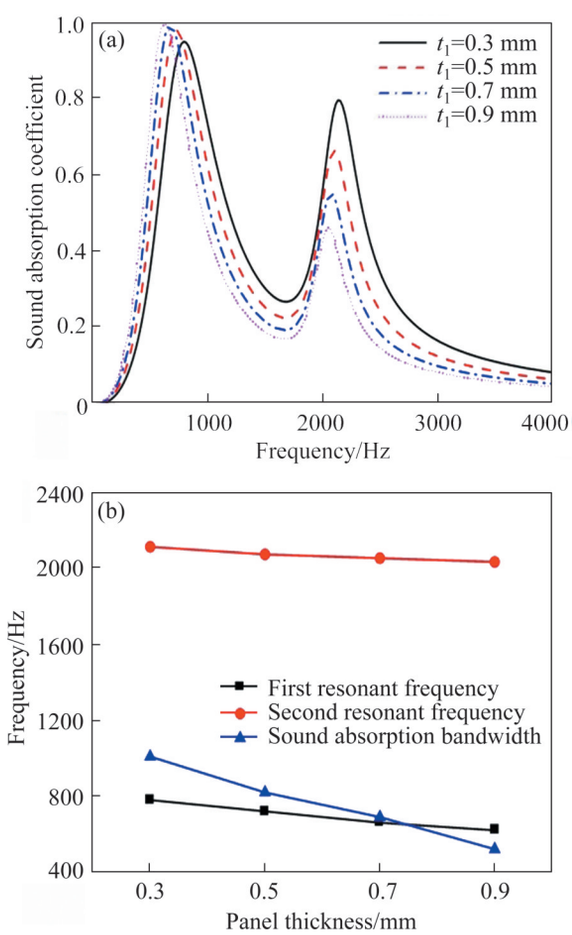

Figure 8 Influences of thickness of front MPP on SAC (theory): (a) Frequency–SAC; (b) Effects of panel thickness on resonant frequency and bandwidth

As shown in Figure 9(a), the changes in the SAC of the double-layer structure with different thicknesses of the back MPP are like that with different orifice diameters of the back MPP. The amplitude of the second peak of the SAC increases with increasing thickness of the back MPP. The first peaks of the SAC all exceed 0.98, and are only slightly influenced by the change of the thickness of the back MPP. Figure 9(b) shows the influences of the thickness of the back MPP on the resonant frequency and bandwidth of the double-layer structure.

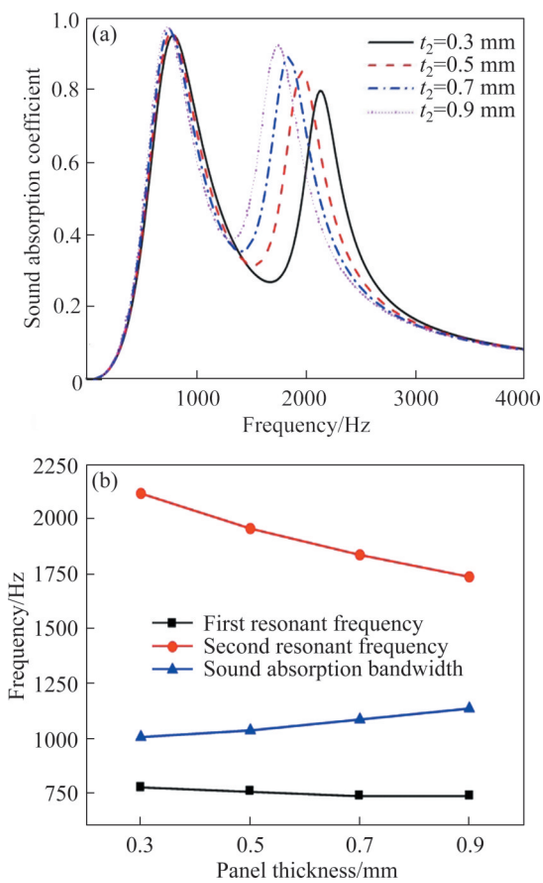

Figure 9 Influences of thickness of back MPP on SAC (theory): (a) Frequency–SAC; (b) Effects of panel thickness on resonant frequency and bandwidth

The thickness of the back MPP mainly affects the second resonant frequency, which decreases with the increasing thickness thereof. Furthermore, the first resonant frequency decreases only slightly with the increase in the thickness of the back MPP. The second peak of the SAC increases when increasing the thickness of the back MPP and thus the sound absorption bandwidth of the double-layer structure increases globally.

3.3 Influences of side length *l* of honeycomb core on SAC

The other fixed geometric parameters of the structures are such that d_1=0.7 mm, d_2=0.6 mm, $t_1=t_2$ =0.3 mm, and D=20 mm. In Figure 10(a), we can compare the curves of the SAC of the double-layer structure with different side lengths of the honeycomb core. The first peak of SAC increases while the second peak of the SAC decreases with the growth of the side length of the honeycomb core. Figure 10(b) demonstrates the influences of the side length of the honeycomb core on the resonant frequency and bandwidth of the double-layer structure. The two resonant frequencies of the structure reduce with increasing side length. With increasing side length, the sound absorption bandwidth of the first peak of SAC decreases and the second peak of SAC of the structure also decreases. Due to the two changes, the global sound adsorption bandwidth of the structure is significantly reduced.

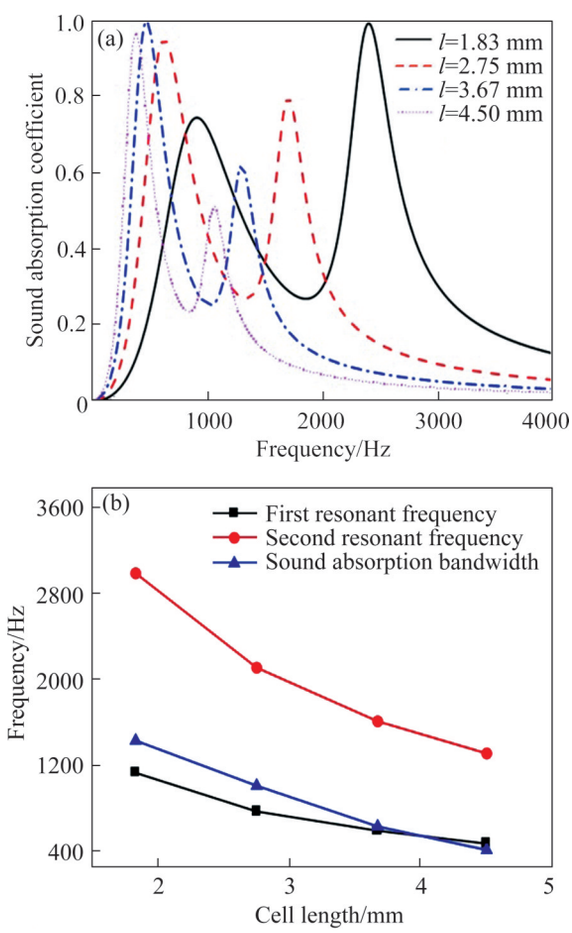

Figure 10 Influences of side length of honeycomb core on SAC (theory): (a) Frequency−SAC; (b) Effects of side length of honeycomb core on resonant frequency and bandwidth

4 Optimization of double-layer honeycomb sandwich panel by genetic algorithm

From the aforementioned results, the sandwich structure can be seen to provide favorable SAP. Based on the model, the structure can be optimized for use in aerospace, railway vehicle, and building applications to improve their noise reduction performance; because the structure consisting of the honeycomb core and MPPs exhibits sufficient mechanical strength and low mass, it can be applied as acoustic shielding, furthermore, the structure is optimized aiming at noise outside trains when used in urban rail transit systems.

The main noise frequency outside such trains is between 400 and 2500 Hz, which is within the sound-absorption range of the double-layer structure designed in the study. The assessment of SAP of the double-layer structure mainly focuses on the SAC and bandwidth of the structure. To design a structure with a better sound adsorption effect, it is necessary to maximize both the SAC and bandwidth of the structure.

4.1 Establishment of mathematical optimization model

At first, it is necessary to establish an optimization model for the double-layer honeycomb sandwich panel. This model is based on a genetic algorithm (GA) and consists of three parts: design variables, a fitness function, and constraints. Aiming at the previous research results, although the side length of the honeycomb core significantly influences all indices affecting the SAP, it is quite difficult to change the side length during machining as it is set according to a certain specification during its production, therefore, in terms of the design variables, the orifice diameters (d_1 and d_2) and thicknesses (t_1 and t_2) of front and back MPPs are considered. Moreover, the orifice diameter of the front MPP is no smaller than that of the back MPP, that is, $d_1 \geqslant d_2$. Aiming at the main noise frequency outside trains within the range of 400 to 2500 Hz, the two resonant frequencies of the double-layer

structure are within that range. The range of the design variables is therefore:

$$\begin{cases} 0.1\,\text{mm} \leqslant d_1 \leqslant 1\,\text{mm} \\ 0.1\,\text{mm} \leqslant d_2 \leqslant 1\,\text{mm} \\ 0.2\,\text{mm} \leqslant t_1 \leqslant 1\,\text{mm} \\ 0.2\,\text{mm} \leqslant t_2 \leqslant 1\,\text{mm} \\ d_1 \geqslant d_2 \end{cases} \tag{17}$$

As shown in Figure 11, the main factors influencing the SAP of the double-layer honeycomb sandwich panel include the first and second peaks of the SAC, the SAC at the wave trough and the distance between two peaks. The two larger peaks of SAC can guarantee the structure offers favorable sound absorption at two frequencies at least; a larger SAC at the wave trough can ensure the SAP of the structure within a wide frequency-band; the greater the distance between the two peaks of SAC, the wider the sound absorption bandwidth of the structure. During optimization, the noise frequency range is below 4000 Hz and the four optimization objectives are calculated according to four design variables.

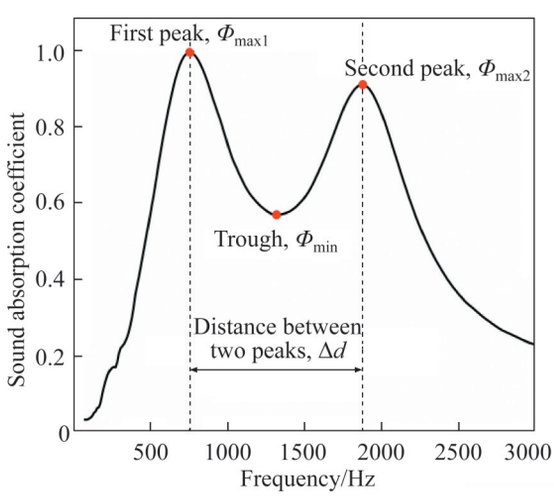

Figure 11 Objectives of fitness function

The aforementioned parameters are taken as the objectives of the fitness function, as given by:

$$\text{Max:}\,[\,\Phi_{max1}, \Phi_{max2}, \Phi_{min}, \Delta d\,] = F\,(d_1, d_2, t_1, t_2) \tag{18}$$

4.2 Analysis of optimization result

A multi-objective GA is applied, with populations of 200 and 400 iterations, and a crossover probability of 0.8. The mutation probability is calculated by using the adaptive method. According to the Pareto front (set of pareto solutions) in Figure 12, the distance between two peaks is negatively correlated with the peaks of the SAC. The distance between two peaks is minimized when the two peaks are at their maximum amplitudes.

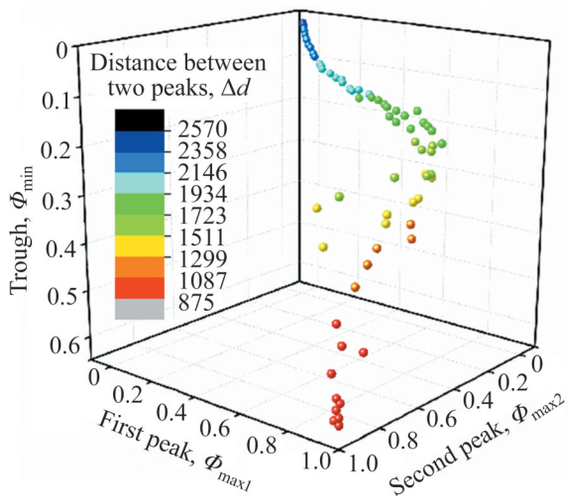

Figure 12 Pareto front (set of pareto solutions)

The peaks of SAC are more important than the distance between the two peaks, therefore, it is possible to select the suitable distance between two peaks and the SAC at the wave trough in condition of guaranteeing the maximization of the peak SAC amplitudes; the resulting optimal parameters are:

$$\begin{cases} d_1 = 0.93\ \text{mm}, \quad d_2 = 0.25\ \text{mm} \\ t_1 = 0.24\ \text{mm}, \quad t_2 = 0.23\ \text{mm} \end{cases} \tag{19}$$

Figure 13 compares the SAC curve under the optimal parameters with the optimal SAC curve during the test. The two peaks of the SAC after the optimization both approximate to 1 and the second peak of SAC is 10% larger than the test result. Moreover, the resonant frequency is lower than that during the test and the optimized structure shows a better SAP within the low-frequency band. The SAC at the wave trough after the optimization is slightly larger than that in the optimal curve during the test while the sound absorption bandwidths differ to a negligible extent. By comparing the main noise frequencies (400 to 2500 Hz) outside such trains, it is found that the main sound absorption frequencies of the structure are within the desired range and the optimized structure can effectively absorb most of the noise generated outside such trains.

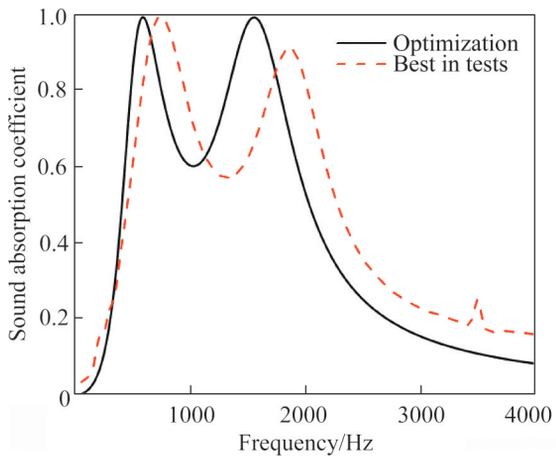

Figure 13 SACs under optimal system parameters

5 Conclusions

To improve the acoustic performance of the honeycomb sandwich panel, the acoustic performance of the original structure was improved using a double-layer structure. AMs composed of a double-layer honeycomb sandwich panel were then designed. The theoretical model of the double-layer structure for sound absorption was established based on the transfer matrix method. Moreover, the dimension parameters of materials and their influences on the SAP of the structure were studied by using an impedance-tube test and a validated theoretical model. Then, the structure was optimized using a GA aiming at the main noise frequencies prevailing outside trains used in urban rail transit systems. The following conclusions were drawn.

1) The thickness and orifice diameter of the front MPP mainly influence the first resonant frequency and the second peak of SAC, both the second peak of SAC and the first resonant frequency decrease when increasing the thickness or decreasing the orifice diameter of the front MPP.

2) The thickness and orifice diameter of the back MPP mainly affect the second resonant frequency and the second peak of SAC, the second peak of SAC increases while the second resonant frequency decreases when increasing the thickness or decreasing the orifice diameter of the back MPP.

3) The side length of the honeycomb core synchronously influences the first and second resonant frequencies as well as two peaks of the SAC. The lower the side length of the honeycomb core, the greater the sound absorption bandwidth while the lower the first peak of the SAC, which influences the SAP of the structure for low-frequency noises. In addition, when the orifice diameter of the front MPP exceeds that of the back MPP, the second peak of the SAC increases to a significant extent, the second resonant frequency is lower, and the sound absorption bandwidth of the structure increases.

4) The optimal values of four design variables (the orifice diameters d_1 and d_2, the thicknesses t_1 and t_2) of the front and back MPPs, were obtained based on optimization by GA. The two peaks of the SAC of the structure under the optimal parameters both tend to 1 and the optimized structure provides an improved SAP for low-frequency noise.

Contributors

WANG Da wrote the original draft, XIE Su-chao helped perform the analysis with constructive discussions, YANG Shi-chen and LI Zhen contributed significantly to manuscript preparation.

Conflict of interest

WANG Da, XIE Su-chao, YANG Shi-chen, and LI Zhen declare that they have no conflict of interest.

References

[1] CAO Lei-tao, FU Qiu-xia, SI Yang, DING Bin, YU Jian-yong. Porous materials for sound absorption [J]. Composites Communications, 2018, 10: 25−35. DOI: 10.1016/j.coco.2018.05.001.

[2] CHEN Chun-yang, LI Wei, LIU You-mei, WEI Xiang. Exploration of key traction-running equipment and its problems on heavy-haul trains and research on technology development [J]. Transportation Safety and Environment, 2020, 2(3): 161−182. DOI:10.1093/tse/tdaa019.

[3] JOSHILKAR M. Analysis of honeycomb structure [J]. International Journal for Research in Applied Science and Engineering Technology, 2018, 6: 950−958. DOI: 10.22214/ijraset.2018.5153.

[4] SHIFA M, TARIQ F, CHANDIO A. Mechanical and electrical properties of hybrid honeycomb sandwich structure for spacecraft structural applications [J]. Journal of Sandwich Structures & Materials, 2019, 23: 1−19. DOI: 10.1177/1099636219830783.

[5] TIAN Hong-qi. Review of research on high-speed railway aerodynamics in China [J] Transportation Safety and Environment, 2019, 1(1): 1−21. DOI:10.1093/tse/tdz014.

[6] TOYODA M, SAKAGAMI K, TAKAHASHI D,

MORIMOTO M. Effect of a honeycomb on the sound absorption characteristics of panel-type absorbers [J]. Applied Acoustics, 2011, 72(12): 943−948. DOI: 10.1016/j.apacoust.2011.05.017.

[7] CHENG Yang, LI Cheng. Sound absorption of microperforated panels inside compact acoustic enclosures [J]. Journal of Sound and Vibration, 2016, 360: 140−155. DOI: 10.1016/j.jsv.2015.09.024.

[8] SAKAGAMI K, YAMASHITA I, YAIRI M, MORIMOTO M. Sound absorption characteristics of a honeycomb-backed microperforated panel absorber: Revised theory and experimental validation [J]. Noise Control Engineering Journal, 2010, 58(2): 157−162. DOI: 10.3397/1.3294861.

[9] LIN Jia-horng, LIN Chin-mei, HUANG Chao-chiung, LIN Chia-chang. Evaluation of the manufacture of sound absorbent sandwich plank made of PET/TPU honeycomb grid/PU foam [J]. Journal of Composite Materials, 2011, 45(13): 1355−1362. DOI: 10.1177/0021998310381438.

[10] YANG Yong, LI Bin-bin, CHEN Zhao-feng, SUI Ni. Acoustic properties of glass fiber assembly-filled honeycomb sandwich panels [J]. Composites Part B: Engineering, 2016, 96: 281−286. DOI: 10.1016/j.compositesb.2016.04.046.

[11] XIE Su-chao, YANG Shi-chen, YANG Cheng-xin, WANG Da. Sound absorption performance of a filled honeycomb composite structure [J]. Applied Acoustics, 2020, 162: 107202. DOI: 10.1016/j.apacoust.2019.107202.

[12] COX T, D'ANTONIO P. Acoustic absorbers and diffusers: Theory, design and application [M]. Boca Raton: CRC Press, 2009. DOI: 10.1121/1.1861060.

[13] ZHAO Dan, WANG Bing, JI Chen-zhen. Geometric shapes effect of in-duct perforated orifices on aeroacoustics damping performances at low Helmholtz and Strouhal number [J]. The Journal of the Acoustical Society of America, 2019, 145(4): 2126−2126. DOI: 10.1121/1.5096642.

[14] MAA D Y. Potential of microperforated panel absorber [J]. The Journal of the Acoustical Society of America, 1998, 104: 2861−2866. DOI: 10.1121/1.423870.

[15] SAKAGAMI K, YAMASHITA I, YAIRI M, MORIMOTO M. Effect of a honeycomb on the absorption characteristics of double-leaf microperforated panel (MPP) space sound absorbers [J]. Noise Control Engineering Journal, 2011, 59: 363−371. DOI: info:doi/10.3397/1.3601762.

[16] SAKAGAMI K, FUKUTANI Y, YAIRI M, MORIMOTO M. A theoretical study on the effect of a permeable membrane in the air cavity of a double-leaf microperforated panel space sound absorber [J]. Applied Acoustics, 2014, 79: 104−109. DOI: 10.1016/j.apacoust.2013.12.015.

[17] BECK B, SCHILLER N, JONES M. Impedance assessment of a dual-resonance acoustic liner [J]. Applied Acoustics, 2015, 93: 15−22. DOI: 10.1016/j.apacoust.2015.01.011.

[18] REGNIEZ M, GAUTIER F, PEZERAT C, PELAT A. Acoustic impedance of microperforated honeycomb panels [C]// Medyna 2013. Marrakech, Morocco, 2013.

[19] PENG X, JI J, JING Y. Composite honeycomb metasurface panel for broadband sound absorption [J]. The Journal of the Acoustical Society of America, 2018, 144: 255−261. DOI: 10.1121/1.5055847.

[20] XIE Su-chao, WANG Da, FENG Zhen-jun, YANG Shi-chen. Sound absorption performance of microperforated honeycomb metasurface panels with a combination of multiple orifice diameters [J]. Applied Acoustics, 2020, 158(1): 107046.1−107046.9. DOI: 10.1016/j.apacoust.2019.107046.

[21] CHANG D, LU F, JIN W, CHANG Dao-qing, LU Fu-an, JIN Wei-nan, LIU Bi-long. Low-frequency sound absorptive properties of double-layer perforated plate under grazing flow [J]. Applied Acoustics, 2018, 130: 115−123. DOI: 10.1016/j.apacoust.2017.09.016

[22] JONZA J, HERDTLE T, KALISH J, GERDES R. Acoustically absorbing lightweight thermoplastic honeycomb panels [J]. SAE International Journal of Vehicle Dynamics, Stability, and NVH, 2017, 1: 445−454. DOI: 10.4271/2017-01-1813.

[23] GUAN Di, ZHAO Dan, LI Jun-wei, CHEN Yong. Aeroacoustic damping performance studies on off-axial double-layer in-duct orifices at low Mach and Helmholtz number [J]. Applied Acoustics, 2019, 156: 46−55. DOI: 10.1016/j.apacoust.2019.06.018.

[24] YANG Xiao-cui, BAI Pan-feng, SHEN Xin-min, TO S. Optimal design and experimental validation of sound absorbing multilayer microperforated panel with constraint conditions [J]. Applied Acoustics, 2019, 146: 334−344. DOI: 10.1016/j.apacoust.2018.11.032.

[25] BAI Pan-feng, YANG Xiao-cui, SHEN Xin-min, ZHANG Xiao-nan. Sound absorption performance of the acoustic absorber fabricated by compression and microperforation of the porous metal [J]. Materials & Design, 2019, 167: 1−14. DOI: 10.1016/j.matdes.2019.107637.

[26] ZHAO D, SUN Y, NI S, JI Chen-zhen. Experimental and theoretical studies of aeroacoustics damping performance of a bias-flow perforated orifice [J]. Applied Acoustics, 2019, 145: 328−338. DOI: 10.1016/j.apacoust.2018.10.025.

[27] HUANG Si-bo, ZHOU Zhi-ling, LI Dong-ting, LIU Tuo. Compact broadband acoustic sink with coherently coupled weak resonances [J]. Science Bulletin, 2020, 65(5): 373−379. DOI: 10.1016/j.scib.2019.11.008.

[28] ZHANG Chi, HU Xin-hua. Three-dimensional single-port labyrinthine acoustic metamaterial: Perfect absorption with large bandwidth and tunability [J]. Phys Rev Applied, 2016, 6(6): 064025. DOI: 10.1103/PhysRevApplied.6.064025.

[29] HUANG Si-bo, FANG Xin-sheng, WANG Xu, ASSOUAR B. Acoustic perfect absorbers via Helmholtz resonators with embedded apertures [J]. The Journal of the Acoustical Society of America, 2019, 145(1): 254−262. DOI: 10.1121/1.5087128.

(Edited by FANG Jing-hua)

中文导读

由双层蜂窝结构构成的声学超材料的吸声性能

摘要：本文研究了每个蜂窝单元上都对应有微穿孔的双层Nomex蜂窝构成的声学超材料的吸声性能。基于传递矩阵法构建理论模型并进行试验测试和验证，研究结构参数对其吸声性能的影响，并基于遗传算法优化了夹层板结构。研究结果表明，面板厚度和孔径主要影响结构第二个共振频率和吸声峰值的大小，胞元大小影响第一、第二共振频率和峰值的大小，过小的蜂窝芯边长会降低结构对低频的吸声性能。同时发现前板孔径大于后板孔径时，结构表现出更好的吸声性能。对列车车外噪声频率进行优化后，结构具有更好的降噪性能。

关键词：声学超材料；吸声；蜂窝夹层板；微穿孔板